

PHYSICAL REVIEW B

CONDENSED MATTER

THIRD SERIES, VOLUME 43, NUMBER 6

15 FEBRUARY 1991-II

Photoabsorption spectra of sodium clusters

Kathy Selby, Vitaly Kresin, Jun Masui,* Michael Vollmer,[†] Walt A. de Heer,[‡] Adi Scheidemann, and W. D. Knight

Department of Physics, University of California, Berkeley, California 94720

(Received 3 August 1990)

Absolute photoabsorption cross sections of free neutral sodium clusters containing from $N = 3$ to 40 atoms are presented. Investigation of a wide continuous range of cluster sizes reveals the size development of the photoabsorption behavior. In the smallest clusters the absorption is moleculelike. A transition to collective electronic excitations (surface plasmons) occurs in the size range of $N = 3$ to 5. For clusters with $N = 6$ to 12 atoms the surface plasma resonances are particularly well defined, and their positions are consistent with the predictions of an ellipsoidal shell model. The cluster shapes can be deduced from the observed resonance positions; the data provide a sensitive measurement of the relative axis lengths of ellipsoidal clusters. For clusters containing $N \gtrsim 3$ atoms, the plasma resonances do not always coincide with the positions predicted by the ellipsoidal shell model. In addition to these resonances, which dominate the spectra, there are three distinct wavelength regions within which absorption occurs for all investigated clusters.

I. INTRODUCTION

Optical spectroscopy provides an elegant means to investigate the underlying electronic structure of clusters. What later became known as "Mie"¹ or "surface plasma" resonances were manifested in the colors of stained glass in medieval times, and investigated as a physical phenomenon in colloidal gold solutions by Faraday.² Many experiments on metal particles embedded in matrices or deposited on surfaces have been carried out since. They have commonly been interpreted in terms of macroscopic theories, employing bulk dielectric functions and including corrections for particle-matrix interactions. More recently, attempts have been made to include quantum size effects (for a review, see Ref. 3). The first investigations of unsupported clusters were made by Mann and Broida.⁴ Later on, optical absorption experiments contributed to understanding the electronic structure of sodium trimers.⁵ Accurate absolute photoabsorption cross sections were recently measured^{6,7} for several mass-selected sodium clusters containing between $N = 8$ and 20 atoms. Peaks in the spectra were identified with surface plasma resonances. This paper discusses photoabsorption measurements on all sodium clusters within the size range of $N = 3$ to 42 atoms. The overall patterns of behavior are examined and are compared with other recent relevant experimental and theoretical work. By investigating a wide continuous cluster size range, trends in photoabsorption behavior are revealed that are not apparent otherwise. Moreover, we are able to distinguish

between absorption features that are unique to a particular cluster size and those that occur for all clusters in a certain size range.

The ellipsoidal shell model (ESM) describes well several properties of simple metal clusters (e.g., relative abundances, ionization potentials,⁸ and electron affinities⁹). We may now ask whether this model will also give good results for cluster photoabsorption. The experiments described here address this, and related, questions. Can the plasma resonances that are well known in solids, on surfaces, and in colloids, be observed in small clusters containing only a few atoms; do the cluster resonance frequencies match those of macroscopic particles; are the multiple plasmon peaks predicted by the ESM observable; will the known static polarizabilities¹⁰ adequately predict the positions of the resonance peaks; and is there evidence for single-particle resonances?

The plan of this paper is given below. In Sec. II the experimental arrangement is outlined. The results are presented in Sec. III, which is laid out as follows. First, we focus on the transition from molecular to collective behavior that occurs in the smallest clusters. Next, the observed surface plasma excitations are discussed. Finally, additional absorption that is seen in all clusters is described. Section IV contains the conclusions.

II. EXPERIMENTAL ARRANGEMENT

The experimental arrangement for the measurement of photoabsorption cross sections is discussed in detail else-

where;^{7,11} a brief description follows. A seeded beam of neutral Na clusters is illuminated by a collinear and counterpropagating laser beam. Photon absorption by a cluster results in the rapid evaporation of one or more atoms, and the subsequent transverse recoil of the daughter cluster prevents it from entering the detector. The evaporation of atoms proceeds sufficiently rapidly compared to the cluster flight time that the probability of detecting a cluster that has absorbed a photon is negligible. This has been demonstrated experimentally: for all investigated clusters ($N \leq 61$), single-photon absorption at elevated laser intensity can deplete the cluster beam to the level of the background noise.¹¹ The photoabsorption cross sections are deduced from the measured beam depletion. In order to measure photoabsorption cross sections

accurately, it is necessary to count only those clusters that were illuminated when they were far from both the source and the detector. The long flight path of our apparatus, combined with a chopped laser beam, allows us to gate the detected cluster signal so that this is achieved. Careful measurements of the photon fluence in the scattering region provide an absolute accuracy of 5–10%.

III. OBSERVATIONS AND DISCUSSION

The photoabsorption spectra of Na clusters containing from $N=3$ to 40 atoms are shown in Figs. 1–4, giving the measured per atom photoabsorption cross sections as a function of wavelength. These data are displayed together

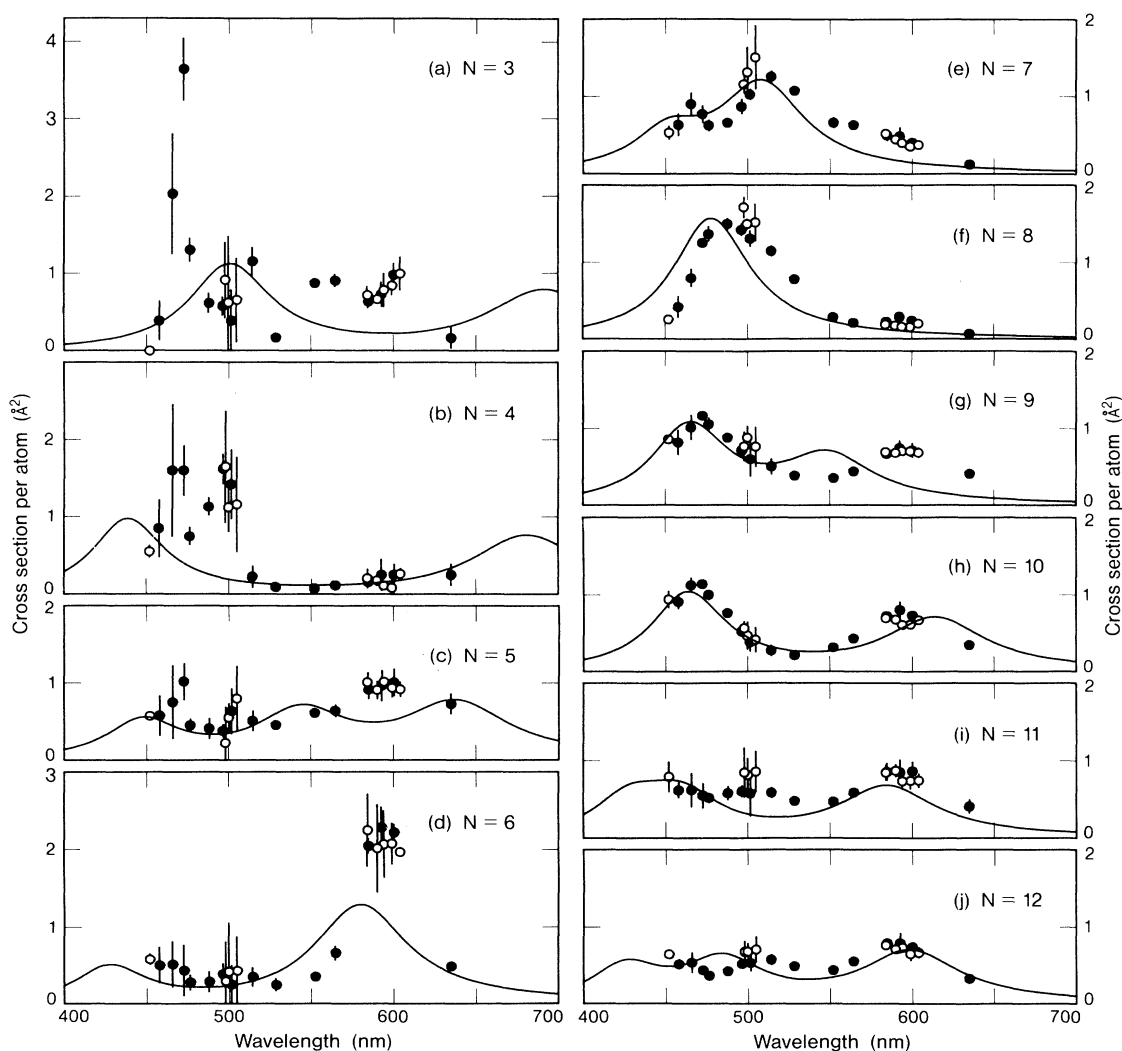


FIG. 1. Experimental (circles) and calculated (solid lines) photoabsorption cross sections vs wavelength for Na clusters of sizes $N=3$ to 12 atoms. The calculated curves each contain 70% of the dipole oscillator strength, and the resonances have relative widths (Ref. 19) of $\gamma=0.12$. These parameters were derived from the best fit of the ESM to the data for Na_8 . The open circles correspond to data taken with a flashlamp laser; the statistical errors in these measurements are about 20%. The data at 498, 500, and 505 nm (open circles) also contain some systematic errors arising from light intensity measurements, and the cross sections at these wavelengths are overestimated by 10% to 35%. The solid circles represent data for which cw lasers were used, and here the statistical errors are from 5% to 10%. The error bars on the data points (which only appear when they are longer than the diameter of the circles) are derived from the experimental scatter between repeated measurements of each point.

er with spectra calculated with the ellipsoidal shell model (ESM) described earlier.^{7,11} This model is outlined in the Appendix.

The photoabsorption behavior falls roughly into three size ranges. For the smallest clusters, moleculelike characteristics are seen, and a transition to collective electronic excitation (surface plasmons) is observed in the size range of $N \approx 3$ to 5 atoms. For $N \approx 6$ to 12, the data correspond quite well to the predictions of the ESM. However, for larger sizes a more complex model is needed.

A. Transition from molecular to collective behavior

Our data, and also photoabsorption measurements by other investigators,^{12,13} indicate that the smallest clusters have moleculelike photoabsorption properties. However, it appears that in the size range of $N = 3$ to 5 atoms, collective electronic resonances begin to dominate the photoabsorption. These resonances have large strengths (see Sec. III B 2), and the strengths *per atom* show a relatively weak cluster-size dependence, as is appropriate for collective excitations.¹⁴ It has long been recognized that collective excitations can occur in systems with a very small

number of particles. Nuclei as small as ^3He exhibit “giant dipole” resonances,¹⁵ and the d shells of transition-metal atoms¹⁴ also undergo collective excitations. Thus it is not surprising to find them in, for example, sodium pentamers.

The photoabsorption spectra for Na_3 and Na_4 each contain several peaks, which are narrower than those seen in the spectra of larger clusters. The Na_5 spectrum profile shows smaller variations as a function of wavelength than are observed for Na_3 and Na_4 (see Fig. 1). This pattern for Na_5 is consistent with the spectrum that one expects from a metal ellipsoid, with three broader peaks representing surface plasmon absorption.

Photoabsorption data obtained by others^{12,13,16} for Na_3 and Na_4 are consistent with our measurements, as discussed below. Na_3 has been investigated^{12,16} by two-photon ionization (TPI) and also by depletion spectroscopy. In that work, photoabsorption occurs in five distinct wavelength regions,¹² corresponding, respectively, to different excited states of Na_3 . Individual vibrational levels are clearly resolved, and the measured energies around 470 nm are in good agreement with calculated values.¹⁶ Our Na_3 photodepletion data show local maxi-

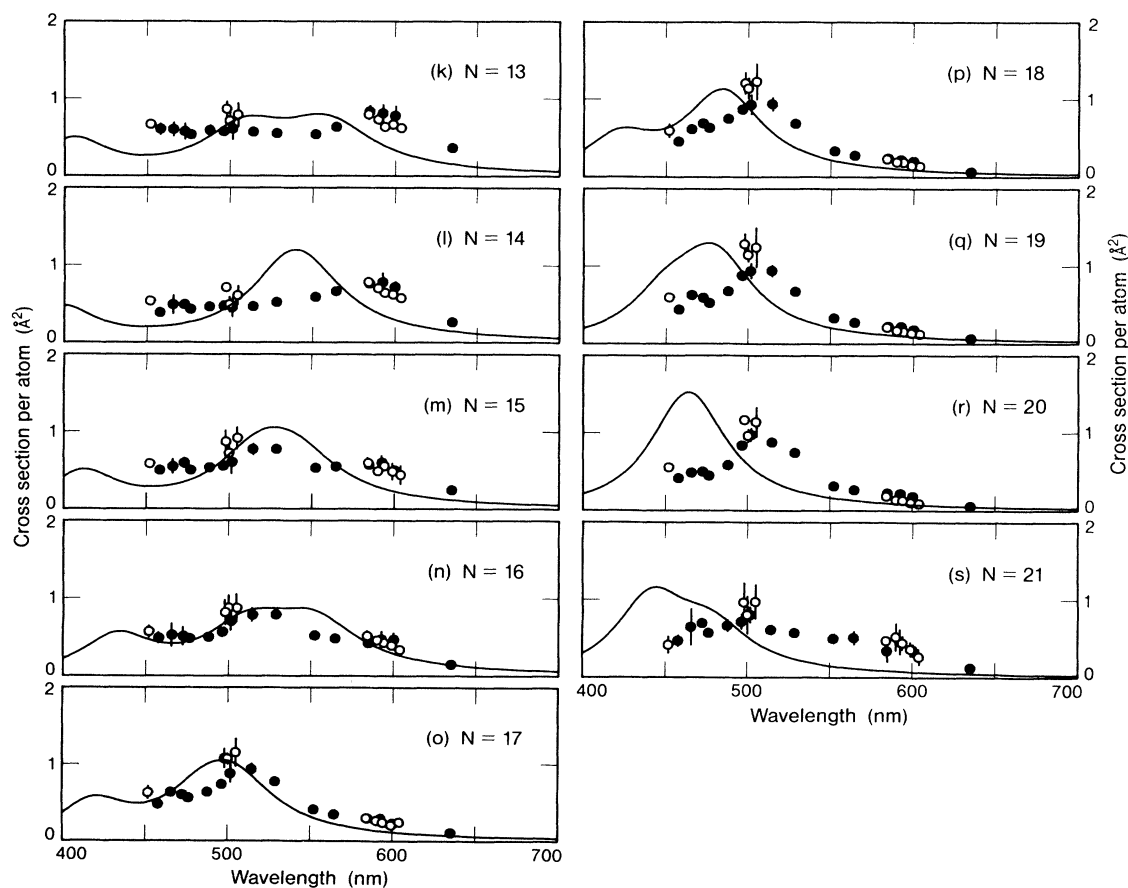


FIG. 2. Experimental (circles) and calculated (solid lines) photoabsorption cross sections vs wavelength for Na clusters of sizes $N = 13$ to 21 atoms. See caption of Fig. 1 for more details.

ma in the cross sections at wavelengths that correspond to large oscillator strengths in the TPI spectrum.¹² We also see relatively strong absorption at 515 nm, where the TPI data show a weaker peak, which is not discussed in Ref. 12. These observed correspondences between the TPI and the photodepletion spectra still require explanation; however, it appears that they both primarily reflect the absorption probability of the first photon. In both TPI and photodepletion experiments, spectra are measured as a function of the wavelength of the first photon, the absorption of which raises the cluster to an excited state. In the TPI method a second photon ionizes the excited cluster, whereas in photodepletion spectroscopy the excited state is allowed to decay, eventually resulting in evaporation of atoms from the cluster.

The photoabsorption spectra of Na₄ measured by us

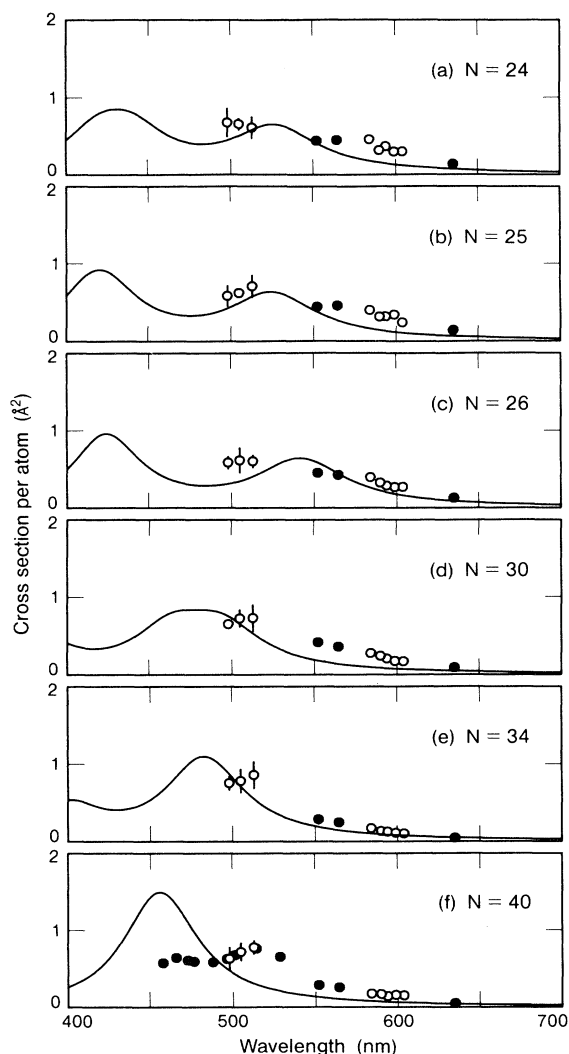


FIG. 3. Experimental (circles) and calculated (solid lines) photoabsorption cross sections for selected Na clusters between $N=24$ and 40. Only those clusters are shown for which the static polarizabilities have been measured (Ref. 10). See caption of Fig. 1 for more details.

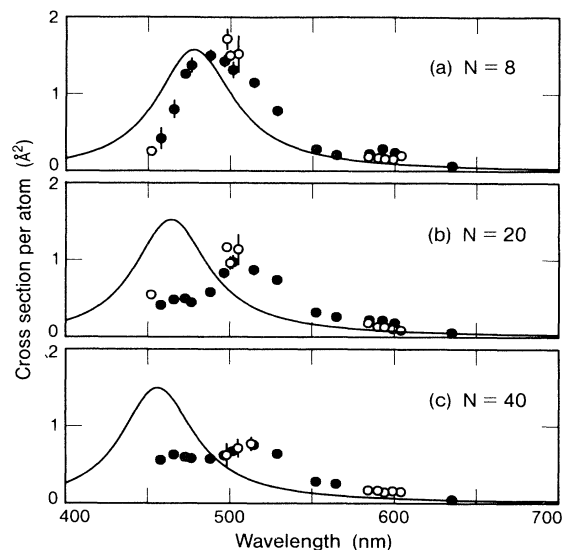


FIG. 4. Experimental (circles) and calculated (solid lines) photoabsorption cross sections vs wavelength for the closed-shell Na clusters $N=8$, 20, and 40. See caption of Fig. 1 for more details.

and by others¹³ show some similarity to the predictions of the ESM, namely two strong resonances occur at 495 and 685 nm.¹³ The high-wavelength peak lies within 1% of the predicted surface-plasma-resonance position, and the position of the low-wavelength resonance differs by 13% from the calculated value. The strength of the low-wavelength peak is about $\frac{3}{2}$ times that of the high-wavelength peak,¹³ while the ESM gives a strength ratio of 2:1. The data also show several smaller peaks. A configuration-interaction calculation¹⁷ finds optically allowed transitions at energies that correspond to those of all of the experimental peaks (see Sec. III B 3).

B. Collective resonances

1. General behavior

For clusters with $N \geq 6$ atoms, the photoabsorption spectra are dominated by broad peaks, as expected for surface plasma resonances. In the size range of $N \approx 6$ to 12, the data are generally in agreement with the ESM (see Fig. 1). The observed surface-plasma-resonance positions reflect the predicted cluster shapes (see the Appendix). Examples of spherical (Na₈), spheroidal (e.g., Na₉ and Na₁₀), and ellipsoidal clusters (e.g., Na₁₂) are seen. The calculated ratios of axis lengths (axial ratios) of clusters^{7,11} strongly affect the position of the predicted resonance peaks, and it is thus not surprising that the predicted resonance positions do not always correspond perfectly with the observed peaks. The experimental resonance positions provide a sensitive measure of the cluster shapes (see Sec. III B 2), and they differ by $< 8\%$ from the predicted values for all clusters in this size range.

For clusters containing from $N \approx 13$ to 21 atoms (see Fig. 2), the photoabsorption behavior partly follows the

ESM, but this model alone is not adequate to explain the data. The data for Na_{13} and Na_{14} deviate furthest from its predictions, as the relatively flat spectra do not show the expected surface plasmon peaks. The measured spectra for $N=15$ through 20 appear more similar to the model: for Na_{15} and Na_{16} the largest experimental cross sections occur in the neighborhood of the calculated resonances, and for $N=17$ to 20 each experimental spectrum is dominated by a single resonance at a wavelength $\approx 5\text{--}10\%$ longer than the corresponding ESM position.

The surface plasma resonances in metal clusters are expected (on average) to move to shorter wavelengths as the cluster size increases. This is because the spillover of the valence electrons outside the boundary of the positive ion cores becomes relatively less important for larger clusters. This effect is seen in both the measured and calculated spectra in Figs. 1–3: for clusters with $N < 13$ atoms, resonances are both predicted and observed at wavelengths as long as 600 nm. However, for the largest investigated clusters (with $N=22$ to 42), the surface-plasma-resonance peaks are all predicted to occur below 550 nm. The experimental photoabsorption spectra for all clusters in the size range of $N=22$ to 42 are very similar (see Fig. 3), in that the cross sections are largest near 500 nm, and all wavelengths above 550 nm are on the long-wavelength tails of the photoabsorption spectra.

Following a spherical shell closing, the observed photoabsorption spectrum profile changes in character. Due to its nonspherical shape, the absorption strength in a closed-shell-plus-1-atom cluster is divided between the multiple surface plasmon peaks. This results in spectrum profiles for which the strength is distributed over a wider wavelength region than for the neighboring closed-shell cluster, which is spherical.

2. Cluster shapes, oscillator strengths, and resonance widths

From the observed photoabsorption spectra, the cluster shapes (spheres, spheroids, or ellipsoids) can be deduced; the experimental resonance positions provide an accurate measure of the relative axis lengths of clusters. In the ESM (see the Appendix) the calculated axial ratios of ellipsoidal clusters are used to predict the surface-plasma-resonance wavelengths. Conversely, one may also work backwards through the model, and use the measured resonance wavelengths to deduce the axial ratios of clusters. Results for Na_9 and Na_{10} are shown in Table I.

TABLE I. Experimental resonance wavelengths for the spheroidal clusters Na_9 and Na_{10} . The corresponding axial ratio of each cluster (defined as the ratio of the lengths of the polar axis and equatorial axis) is deduced from these resonance positions.

N	Experimental resonance wavelengths (nm)			Axial ratio
9	594	471	→	1.46
10	593	469	→	1.47

TABLE II. Axial ratios calculated with the ESM (see the Appendix) for Na_9 and Na_{10} , together with the resonance wavelengths that are deduced from them. For Na_{10} , the axial ratio and resonance wavelengths calculated by Ekardt and Penzar (Ref. 18) are also shown.

N	Name of model	Axial ratio	Calculated resonance wavelengths (nm)
9	ESM	1.31 →	549 465
10	ESM	1.57 →	614 464
10	Ekardt and Penzar	1.63	588 428

The observed spectra for these clusters each contain two resonance peaks, with an experimentally estimated oscillator strength ratio of 2:1, as expected for prolate spheroids [see Figs. 1(g) and (h)]. The two observed spectra are very similar, with little difference between their resonance positions. This is reflected in the similarity of the axial ratios obtained.

For comparison, axial ratios calculated with the ESM (as described in the Appendix) for Na_9 and Na_{10} are shown in Table II, together with the resonance wavelengths deduced from them. These axial ratios differ by 10% and 7%, respectively, from the values obtained from the experimental resonance positions (see Table I). Ekardt and Penzar¹⁸ have used a self-consistent spheroidal jellium model to calculate the photoabsorption spectrum of Na_{10} , and their results are also shown in Table II. Their calculated resonance positions and axial ratio differ by $< 10\%$ from the corresponding measured values, with both calculated resonance positions appearing at shorter wavelengths than experiment.

For $N=8, 9$, and 10, a curve-fitting procedure was used to estimate the relative widths¹⁹ of the observed surface plasma resonances and the total oscillator strengths accounted for by the measured spectra, as shown in Table III.

The observed surface plasma resonances have relative widths¹⁹ of about $\gamma \approx 0.12$ for most investigated clusters; it has been proposed that these widths are mainly due to the coupling of the electrons with thermal fluctuations of

TABLE III. The relative widths and total oscillator strengths of Lorentzians fitted to the surface-plasma-resonance peaks of Na clusters with $N=8, 9$, and 10 atoms. The data for Na_9 and Na_{10} were least-squares fitted to a sum of two Lorentzians [both with the same relative width (Ref. 19), γ], the lower wavelength peak having twice the strength of the higher peak. For Na_8 , a single Lorentzian was used. The free parameters in the fits were the resonance wavelengths, the relative widths, and the total oscillator strengths of the fitted curves. The total oscillator strengths are shown in the table as a percentage of the total dipole oscillator strength of the cluster valence electrons.

N	Relative width γ	Strength
8	0.12 ± 0.01	$(70 \pm 5)\%$
9	0.12 ± 0.01	$(75 \pm 5)\%$
10	0.09 ± 0.01	$(60 \pm 5)\%$

the cluster shapes.^{20–22} This mechanism implies a temperature dependence of the width, which is found to be $\Gamma \sim \sqrt{T}$. For clusters at a temperature $T = 290$ K, which is a best estimate for our apparatus (see footnote 16 in Ref. 21), the calculated widths²¹ are consistent with the measurements. Interaction of the collective modes with single-electron excitations may also contribute to the observed widths.^{23,24}

The ESM assumes that surface plasmons account for all of the oscillator strength represented by the dipole sum rule (see the Appendix). However, the data account for between 85% (for the peak at 590 nm in Na₆) and an estimated 40% (in Na₄₀) of the dipole strength, with a general decrease in the *per atom* strength with increasing cluster size. This implies that additional absorption occurs outside of the investigated wavelength range (see Sec. III B 3). Nevertheless, the observed resonance peak positions for clusters with $N = 6$ to 12 atoms are in reasonable agreement with the calculation.

3. Sum rules: Accounting for missing oscillator strength

The data for the closed-shell clusters Na₈, Na₂₀, and Na₄₀ (see Fig. 4) are particularly useful for comparison with theory; their predicted spherical geometry simplifies the calculations. The ESM predicts only one surface plasmon peak for spherical clusters; the Na₈ data are closest to this expectation. A resonance is observed at 492 ± 3 nm, within 3% of the calculated value^{7,11} of 478 ± 4 nm. A second, much smaller peak is situated at 590 nm. Another Na₈ photoabsorption spectrum¹³ (see below) is very similar to ours, showing a strong resonance at 490 nm and a much weaker peak around 590 nm. The measured oscillator strengths are stated to be accurate to 50%.¹³ The relative width of the main peak is $\gamma = 0.09$, which is smaller than our observed value. This difference remains to be explained.

We find for Na₂₀ that there is a peak at 505 ± 5 nm. A trend of increasing cross sections at the lowest investigated wavelengths suggests the possibility of a second peak below 450 nm for this cluster.¹³

A study by Yannouleas *et al.*²⁴ may explain the dominant experimental features for Na₈ and Na₂₀. Single-particle states lying close to the surface plasmon are expected to couple strongly to it, causing a splitting (“fragmentation”) of the plasma resonance (see also Ref. 25). In both of these clusters, the total resulting collective absorption is calculated²⁴ to account for about 75% of the dipole oscillator strength, and the remainder is taken up by single-electron excitations. For Na₈, a single collective resonance is predicted at 441 nm, which is somewhat shorter than experiment. The predicted oscillator strength for this cluster is in agreement with the measured value of $(70 \pm 5)\%$. For Na₂₀, the calculation gives two closely spaced collective excitations, at 426 and 475 nm. The strength of the higher wavelength peak is consistent with that of the observed peak at 505 nm.

This calculation²⁴ indicates that a major factor in determining whether observed photoabsorption spectra will conform to the ESM (which does not predict

surface plasmon fragmentation) is the proximity of the surface plasmon to single-electron levels. In charged potassium clusters, the experimental spectra²⁶ show no evidence for fragmentation. Yannouleas *et al.* calculate that the relevant single-electron states in charged clusters are much higher in energy than the surface plasmon,^{24,27} with consequently reduced coupling and fragmentation.

Kresin predicts that the photoabsorption strength in neutral spherical Na clusters is shared between a surface- and a volume-plasma resonance.²⁸ For Na₈ the surface-plasma resonance occurs at 493 nm,²⁹ and accounts for 78% of the dipole oscillator strength.²⁸ This resonance position is in excellent agreement with the data, and the calculated strength is also in agreement with the measured value. Throughout the experimentally investigated cluster size range of $N \leq 42$ atoms, the volume plasma resonance is expected to occur at about 280 nm. Neither volume plasmons nor single-particle excitations (predicted by Yannouleas *et al.*; see above) have yet been identified experimentally.

These calculations by Yannouleas *et al.* and Kresin are essentially based on the jellium model. Using the different approach of *ab initio* solution of the many-body Hamiltonian, Bonačić-Koutecký *et al.*^{17,30} have calculated the optically allowed transitions of Na₄ and Na₈. For both Na₄ and Na₈, several transitions are predicted^{17,30} to occur within the experimentally investigated wavelength range. Their positions are within 5% of the observed peaks,¹³ and the calculated relative oscillator strengths are consistent with experiment. For Na₈, one of the possible atomic configurations gives transitions near 490 nm (i.e., corresponding to the strongest observed peak) which account for 66% of the dipole oscillator strength.³⁰ This value is compatible with our measured value of $(70 \pm 5)\%$. The agreement with experiment of the *ab initio* method^{17,30} does not imply that surface plasmons do not exist in clusters. We believe that some of the calculated eigenstates may be characterized as surface plasmons.

C. Spectral features common to all cluster sizes

In three different wavelength regions, enhanced absorption occurs in most of the experimental spectra in the size range from $N = 3$ to 21 atoms. At (i) 450–475 nm, (ii) 500–520 nm, and (iii) 585–605 nm, the spectra contain either a peak, or a “bump” (i.e., the data points lie higher than the simplest curve through the spectrum; for example, at 590 nm in the data for Na₈). These three wavelength regions each lie close to an observed transition in, respectively, Na dimers,³¹ trimers,¹² and atoms³² (the Na *D* lines), and it is worth questioning whether this correspondence may be more than mere coincidence. For some clusters, one or more of these regions may overlap with an observed surface plasma resonance. In these cases it is not possible to distinguish between surface plasma absorption and other possible excitations that may be enhancing the strength of the observed peak.

Similar correspondences are also seen in the data for clusters with $N = 22$ to 42 atoms. For all clusters in this size range, the cross sections are largest near 500 nm.

For most of the clusters with $22 \leq N \leq 30$, there is a broad "bump" centered around 560–590 nm (this feature is not seen for $N > 30$).

Among all investigated clusters, the strongest observed resonance occurs around 590 nm for Na_6 , accounting for $(85 \pm 15)\%$ of the dipole oscillator strength. The peak lies within 2% of the wavelength of 580 nm predicted by the ESM. Na_6 is expected to be an oblate spheroid, and this resonance should account for a maximum of $\frac{2}{3}$ (i.e., 67%) of the total oscillator strength; its unusual strength may result from the absorption enhancement that is seen in most clusters near 590 nm.

The measured photoabsorption spectrum of Cs_8 clusters³³ has a line shape similar to that observed for Na_8 , showing one strong peak and a weaker peak at a longer wavelength. For both Cs_8 and Na_8 , the weaker peak (at 832 nm in Cs_8 and at 590 nm in Na_8) lies close to the corresponding atomic resonance³² (852 nm for Cs). As mentioned above, enhanced absorption near the Na atomic resonance is seen in the spectra of most Na clusters. These observations suggest that absorption by individual atoms within the clusters may influence the observed spectra.

IV. SUMMARY AND CONCLUSIONS

Photoabsorption spectra are presented for neutral sodium clusters containing from $N=3$ to 40 atoms. The measurements provide accurate cross sections for a wide continuous range of cluster sizes, enabling us to analyze the size evolution of the spectra.

Although the results for the smallest clusters ($N=3,4$) can be well described within a molecular framework, some of the observed peaks correspond to predictions of the ellipsoidal shell model (ESM). In the size range of $N=3$ to 5, a transition occurs from this moleculelike behavior to collective motion of the delocalized valence electrons. The spectra of clusters with five or more atoms display broad surface plasma resonances that account for from $\approx 40\%$ to 80% of the dipole-oscillator-strength sum rule. The resonance frequencies are significantly redshifted from those for macroscopic particles, reflecting the spillout of the valence electrons, which effectively reduces the electron density in small clusters.

For clusters with $N \approx 6$ to 12 atoms, the data are adequately described by the ESM, and the positions of the collective resonances provide a sensitive measurement of cluster distortions. For $N=13$ to 42, the experimental peak positions do not always coincide with the predictions of this model, and the resonances account for less oscillator strength per atom than in the smaller clusters. These observations may be due to a coupling of the surface plasmon with single electron excitations, resulting in fragmentation of the collective peaks. The ESM, which makes use of the experimentally determined static electric polarizabilities of clusters to predict the resonance frequencies, necessarily fails to describe the dynamic behavior when it is complicated by couplings between the different modes of electronic excitation.

The observed peaks have widths of about 8–15% of the resonance frequencies for all investigated clusters; the

narrower peaks occur mainly in the smallest clusters, with $N \leq 6$ atoms. The measured widths for all sizes are consistent with a broadening mechanism due to thermal fluctuations of the cluster shapes; other effects (for example, the coupling of electrons to ionic vibrations and the escape of photodissociated cluster fragments into the continuum) may also contribute. The experimental widths for these small clusters are comparable to observed surface plasmon widths in bulk metals.³⁴ For the latter, direct measurements of surface plasmon energy loss³⁵ show the importance of the interaction between electronic and surface vibrations.

The resonance positions and widths of the observed peaks clearly show that the surface plasma resonances seen in macroscopic particles are also present in clusters containing as few as $N=3$ to 6 atoms, representing collective oscillations of the free electrons. It is known that the static polarizabilities of small alkali-metal clusters reflect the electronic screening characteristic of metals. The photoabsorption experiments show that the dynamical response is also metal-like for very small clusters.

ACKNOWLEDGMENTS

We thank Michael Kruger and André Châtelain for their valuable participation in the early stages of the experiments. We are grateful to Eugene Commins, Andrew Kung, and Tetsuo Hadeshi for lending us lasers, and to Conny Carlberg for advice on laser operation. We have benefitted greatly from discussions with Walter Ekaradt, Zlatko Penzar, Constantine Yannouleas, Marvin Cohen, and Steven Louie. This research was funded by the U. S. National Science Foundation, under Grant No. DMR-89-13414. M. V. and A. S. thank the Deutsche Forschungsgemeinschaft for financial support.

APPENDIX A: ELLIPSOIDAL-SHELL-MODEL CALCULATION OF CLUSTER PHOTOABSORPTION SPECTRA

This appendix gives an outline of the ellipsoidal shell model (ESM), which is described in detail in Refs. 7 and 11. Clusters are approximated by ellipsoids, and the valence electrons are assumed to move in an ellipsoidal harmonic-oscillator potential. By minimizing the total electronic energy with respect to the cluster shape, the relative axis lengths of the ellipsoid are obtained. These calculated shapes are used to obtain the surface-plasma-resonance wavelengths, as described below.

The photoabsorption spectrum of an ellipsoidal cluster contains three surface-plasma-resonance peaks, each corresponding to a different axis of the ellipsoid. For spheroidal clusters (where two axes are of equal length), the spectra contain two peaks, one having twice the strength of the other. For spherical clusters, the three resonances are degenerate, and the spectra contain only one peak. It is assumed that these resonances exhaust the dipole sum rule given by³⁶

$$\int_{\omega=0}^{\infty} \sigma(\omega) d\omega = 2\pi^2 \frac{Ne^2}{m_e c} . \quad (\text{A1})$$

Here, $\sigma(\omega)$ is the frequency-dependent photoabsorption cross section, and N is the number of valence electrons in the cluster. Under this assumption, each of the three resonance frequencies, ω_{0i} , is related (see, e.g., Refs. 23 and 37) to the corresponding component of the *static* polarizability of the cluster, α_i :

$$\omega_{0i}^2 = \frac{Ne^2}{m_e \alpha_i} . \quad (\text{A2})$$

The average static polarizabilities of randomly oriented Na clusters have been measured,¹⁰ and the three separate polarizability components can be deduced using the calculated relative axis lengths of the ellipsoid (see above). Thus, using Eq. (A2), the resonance wavelengths in ellipsoidal clusters can be calculated. Each resonance is assumed to have a Lorentzian line shape; the widths are the only free parameters in this model, and may be estimated from the data.

*Permanent address: Department of Physics, Cornell University, Ithaca, NY 14853.

†Permanent address: Physikalisches Institut der Universität Heidelberg, D-6900 Heidelberg 1, Federal Republic of Germany.

‡Permanent address: Institut de Physique Expérimentale, Ecole Polytechnique Fédérale de Lausanne, PHB-Ecublens, CH-1015 Lausanne, Switzerland.

¹C. Mie, *Ann. Phys. (Leipzig)* [Folge 4] **25**, 377 (1908).

²M. Faraday, *Philos. Trans.* **147**, 145 (1857).

³U. Kreibig and L. Genzel, *Surf. Sci.* **156**, 678 (1985).

⁴D. M. Mann and H. P. Broida, *J. Appl. Phys.* **44**, 4950 (1973).

⁵A. Herrmann, M. Hofmann, S. Leutwyler, E. Schumacher, and L. Wöste, *Chem. Phys. Lett.* **62**, 216 (1979).

⁶W. A. de Heer, K. Selby, V. Kresin, J. Masui, M. Vollmer, A. Châtelain, and W. D. Knight, *Phys. Rev. Lett.* **59**, 1805 (1987).

⁷K. Selby, M. Vollmer, J. Masui, V. Kresin, W. A. de Heer, and W. D. Knight, *Phys. Rev. B* **40**, 5417 (1989). In Ref. 7, a typographical error occurred. The sentence following Eq. (8) should read as follows: “ ω_0/x_0 , ω_0/y_0 , and ω_0/z_0 are the oscillator frequencies along the three axes of the ellipsoid, which has normalized axial ratios x_0 , y_0 , and z_0 , respectively.” Also, in Eqs. (8) and (9) the symbol ω_0 does not represent a surface-plasma-resonance frequency, as it does elsewhere in the paper.

⁸W. A. de Heer, W. D. Knight, M. Y. Chou, and M. L. Cohen, in *Solid State Physics*, edited by F. Seitz and D. Turnbull (Academic, New York, 1987), Vol. 40, p. 93.

⁹C. L. Pettiette, S. H. Yang, M. J. Craycraft, J. Conceicao, R. T. Laaksonen, O. Cheshnovsky, and R. E. Smalley, *J. Chem. Phys.* **88**, 5377 (1988).

¹⁰W. D. Knight, K. Clemenger, W. A. de Heer, and W. A. Saunders, *Phys. Rev. B* **31**, 2539 (1985).

¹¹K. Selby, Ph.D. thesis, University of California, Berkeley (1990).

¹²M. Broyer, G. Delacrétaz, Ni Guoquan, J. P. Wolf, and L. Wöste, *Chem. Phys. Lett.* **145**, 232 (1988).

¹³C. R. C. Wang, S. Pollack, and M. M. Kappes, *Chem. Phys. Lett.* **166**, 26 (1990); C. R. C. Wang, S. Pollack, J. Hunter, G. Alameddini, T. Hoover, D. Cameron, S. Liu, and M. M. Kappes, *Z. Phys. D* (to be published).

¹⁴A. Zangwill, in *Giant Resonances in Atoms, Molecules and*

Solids, edited by J. P. Connerade, J. M. Esteve, and R. C. Karnatak (Plenum, New York, 1987), p. 321.

¹⁵B. L. Berman and S. C. Fultz, *Rev. Mod. Phys.* **47**, 713 (1975).

¹⁶M. Broyer, G. Delacrétaz, G.-Q. Ni, R. L. Whetten, J.-P. Wolf, and L. Wöste, *J. Chem. Phys.* **90**, 843 (1989).

¹⁷V. Bonačić-Koutecký, P. Fantucci, and J. Koutecký, *Chem. Phys. Lett.* **166**, 32 (1990).

¹⁸W. Ekardt and Z. Penzar, *Phys. Rev. B* **43**, 1322 (1991).

¹⁹The dimensionless relative width γ is defined as $\gamma = \Gamma/\omega_0$, where Γ is the full width at half maximum of the resonance and ω_0 is the resonance frequency.

²⁰G. F. Bertsch and D. Tománek, *Phys. Rev. B* **40**, 2749 (1989).

²¹J. M. Pacheco and R. A. Broglia, *Phys. Rev. Lett.* **62**, 1400 (1989).

²²Z. Penzar, W. Ekardt, and A. Rubio, *Phys. Rev. B* **42**, 5040 (1990).

²³W. Ekardt, *Phys. Rev. B* **31**, 6360 (1985).

²⁴C. Yannouleas, R. A. Broglia, M. Brack, and P. F. Bortignon, *Phys. Rev. Lett.* **63**, 255 (1989).

²⁵V. Kresin, *Z. Phys. D* (to be published).

²⁶C. Bréchnignac, Ph. Cahuzac, F. Carlier, and J. Leygnier, *Chem. Phys. Lett.* **164**, 433 (1989).

²⁷C. Yannouleas, J. M. Pacheco, and R. A. Broglia, *Phys. Rev. B* **41**, 6088 (1990).

²⁸V. Kresin, *Phys. Rev. B* **42**, 3247 (1990).

²⁹V. Kresin, *Phys. Rev. B* **39**, 3042 (1989).

³⁰V. Bonačić-Koutecký, M. M. Kappes, P. Fantucci, and J. Koutecký, *Chem. Phys. Lett.* **170**, 26 (1990).

³¹M. A. Hennesian, R. L. Herbst, and R. L. Byer, *J. Appl. Phys.* **47**, 1515 (1976).

³²*CRC Handbook of Chemistry and Physics*, 50th ed., edited by R. C. Weast (Cleveland Rubber Co., Cleveland, 1970), p. D-167.

³³H. Fallgren and T. P. Martin, *Chem. Phys. Lett.* **168**, 233 (1990).

³⁴H. Raether, *Excitation of Plasmons and Interband Transitions by Electrons* (Springer, New York, 1980).

³⁵M. van Exter and A. Lagendijk, *Phys. Rev. Lett.* **60**, 49 (1988).

³⁶J. Speth and A. van de Woude, *Rep. Prog. Phys.* **44**, 719 (1981).

³⁷A. A. Lushnikov, V. V. Maksimenko, and A. J. Simonov, in *Electromagnetic Surface Modes*, edited by A. D. Boardman (Wiley, New York, 1982).